

# Energy Flow Modeling of Night Storage Heaters and Its Usage for Sector Coupling

Marc Gennat, Marc.Gennat@hs-niederrhein.de  
Raschad Damati, Raschad.Damati@hs-niederrhein.de  
Arne Graßmann, Arne.Grassmann@hs-niederrhein.de  
Hochschule Niederrhein – University of Applied Science

## Overview

Night storage heaters [4] are still used in Germany and facilitated in the past cheaper electrical energy during the night. In recent years no new installations were made due to higher costs of electrical energy compared to fossil fuels like natural gas and oil, which are commonly used for heating. Moreover, electric heating uses more primary energy compared to e.g. natural gas, due to the losses resulting from the energy conversion of electric power plants using fossil fuels. Nevertheless, night storage heaters are still in use in many apartments, which were built between the 1960s to 1980s. However, night storage heaters can facilitate and contribute some share of reducing greenhouse gas emissions by using electric power for heating in times of surplus renewable energy in the grid instead of using natural gas or other fossil fuels. Additionally, night storage heaters have the potential to allow demand-side-management of electrical energy. Hereby, explicit knowledge of room temperature profiles over time is mandatory.

In this contribution, an approach of modeling temperature profiles and simulating the temperature over time is shown. The used data were derived from a laboratory test room. Several differential equations, which are based on thermodynamically principles, are used for modeling and parameter estimation is used to compute unknown parameters of the differential equations. Finally, the model computes the room temperature based only on the knowledge of electric power and the outside ambient temperature. Parameter estimation computes the maximum deviation of the test room temperature to the measured temperature to 0.96 Kelvin, and average deviation is calculated to 0.21 Kelvin.

With the presented model of energy flow and temperature calculation considering a night storage heater, which is installed in a test room, the switch-on periods over a complete year and given outside ambient temperatures of Düsseldorf in 2017 are predetermined.

In further investigations, additional constraints will be integrated in the model to compute the optimal electrical power switch-on points of time in order to reduce fluctuations in room temperature or minimize electricity procurement costs.

## Climate test environment and measurement setup

For measuring the energy flow and temperature, a test room were built, which corresponds to a model of a living room equipped with a conventional electrical night storage heater, shown in Fig. 1. Built in drywall construction method, the test room is divided into two accessible rooms by a sand-lime brick wall as a model of a common outer wall. One of these rooms corresponds to the actual test area and the other one to a climate area for simulating different environmental conditions. The test area is prepared to analyze different charging strategies for night storage heaters. It is equipped with a four kilowatt electrical night storage heater, controlled by a charging control system. The climate area is equipped with a two kilowatt air conditioning unit providing a cooling range of -5 to 20 degrees Celsius, regulated by a programmable logic controller (PLC).

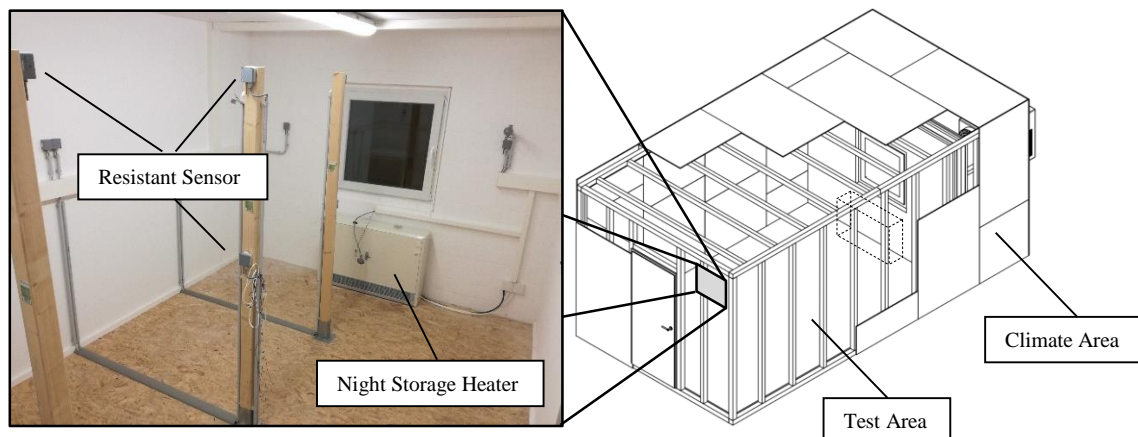
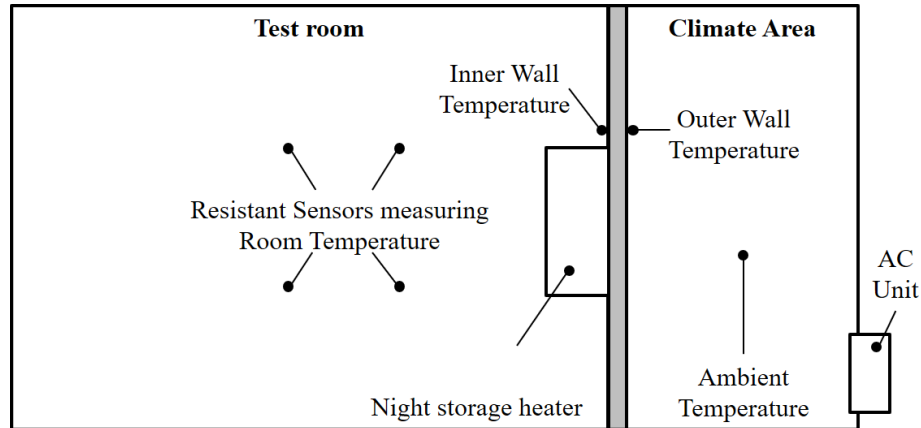


Fig. 1: Test room view and setup

Temperature is measured by multiple resistance sensors in the test area and two resistance sensors in the climate area (Fig. 2). In addition, the surface temperature of the sand-lime brick wall, and the surface temperature of the night storage heater as well as the core temperature and the electrical power consumption of the night storage heater are measured.

To reduce heat losses through the walls, ceiling and floor, they are insulated on test area side with glass wool mats (thermal conductivity  $\lambda = 0.4 \text{ W/mK}$ ,  $th = 80 \text{ mm}$ ) and on climate area side with polyurethane rigid foam panels (thermal conductivity  $\lambda = 0.2 \text{ W/mK}$ ,  $th = 160 \text{ mm}$ ). In addition, all walls are equipped with a steam barrier (0.125 mm) on the warm air side to protect against water vapor diffusion and thus moistening of the insulation layers. Due to the different insulation of existing apartments which are equipped with night storage heater, a direct transfer of the model to real apartments is not possible and an individual parameter estimation for each apartment is required.



**Fig. 2: Test room's schematically representation**

## Reference Scenario

The reference scenario describes a nine-day period with huge steps in average ambient air temperature from one day to the next, which is shown in Fig. 3. In general, huge steps in average ambient air temperature are difficult to handle by night storage heaters, especially, when an old charging control system is used. Those charging control systems calculate the energy demand for the next day based on the local 24-hour-average ambient air temperature of the previous day. Thus, major differences between the ambient air temperature of two consecutive days usually leads to false energy forecast for the electrical night storage heater. Modern charging control systems consider larger periods in past or even utilize weather forecast data to keep the error in forecast as small as possible. Such a charging control system is used in the present investigation.

In general, the 24-hour-average ambient temperature differs from day to day up to six degrees Celsius referring to German Meteorological Service (DWD) weather data from Düsseldorf of the years 2009 to 2017 [2].

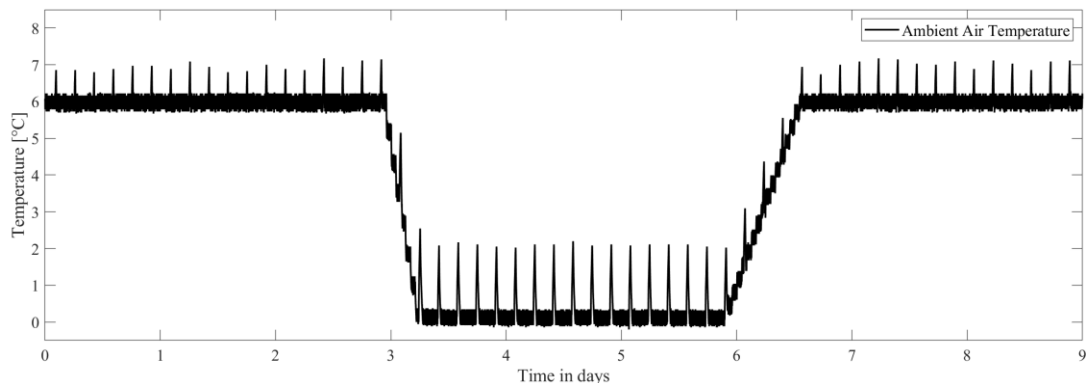


**Fig. 3: Predetermined Ambient Air Temperature during nine Days Test Run**

For this investigation, the ambient air temperature will change from warm to cold after the third day and vice versa from day six to day seven of the nine-day period with about three days of persistence between. For the rates of change in temperature, the above mentioned weather data were analyzed and the local average maximum temperature range  $\Delta T$  and average temporal gradient  $\Delta T / \Delta t$  of weather changes were determined. The resulting course of ambient air temperature is shown in Fig. 3 with upper and lower bounds set to six and zero degrees Celsius. Regular peaks along the curve of ambient air temperature arise from defrosting ceiling cooling unit, which is started automatically about every four hours.

Heating with night storage heaters can be restricted to certain time periods. In the last century, these charging release periods were situated in night times, when electrical power was cheaper, respectively there was a surplus of electrical energy in the power grid. As a default for heating in this given test scenario, charging release periods for the electric night storage heater was set from 10:00 p.m. to 6:00 a.m.

With the given course of ambient air temperature, the measured average charging times amounts to approximately 1 hour and 20 minutes by six degrees Celsius and about 1 hour and 30 minutes by zero degrees Celsius. The decreasing in temperature from six degrees Celsius to zero degrees Celsius in the night between day three and day four leads to a subsequent charging of about 30 minutes at the end of charging release. So the total time of charging in the night between day three and day four amounts to 1 hour and 50 minutes. In contrast, the increasing of temperature from zero degrees Celsius to six degrees Celsius in the night between day six and day seven leads to a significant shorter charging time in the following night of nearly 50 minutes in total. The charging releases at night results in a saw-tooth pattern of room temperature that is typical for operating with electrical night storage heaters. During the nine-day test run the fluctuations in room temperature are measured with approximately 3 Kelvin and moves within the range of 19 degrees Celsius and 22 degrees Celsius.

## Methodology

To compute the room temperature, a thermodynamically approach is applied using the Fouriers' heat conduction law

$$\frac{\partial T}{\partial t} = a \cdot \nabla^2 T = a \cdot \text{div}(\text{grad } T), \quad (1)$$

where  $T$  is the temperature in Kelvin,  $t$  is the time in seconds and  $a$  is the thermal diffusivity in square meters per second. The system to be solved consists of several layers of solid and fluid respectively gaseous materials. This can be solved e. g. by a finite difference approach [5]. A numerical solution for large time scales is very difficult and time consuming, a relaxation of the given problem would increase the effort by orders of magnitude. Additionally, the material properties of all layers must be known exactly to compute  $a$  in (1), which is usually difficult, as manufacturers of night storage heaters do not provide these data. This leads to the result, that classical thermodynamic approaches cannot be applied straight forward to our optimization problem, and a relaxed approach has to be used. Thus, isotropic conditions are assumed, which leads to thermal conductivity equation [3]

$$\dot{q} = -k \nabla T = -k (T_1 - T_2) \text{ with } T_1 > T_2, \quad (2)$$

whereby  $\dot{q}$  represents the energy flux and  $k$  denotes the material's conductivity in watts per Kelvin and meters. In (2)  $T_1$  and  $T_2$  represents the temperatures in an one-dimensional coordinate space, which is shown in Fig. 4. Thus, it is considered, that in this given relaxed examination energy transfer takes place only in the illustrated x-direction, and no energy flow occurs in y- and z-direction. With parameters area  $A_i$  heat transfer  $U_i$  the thermal conductivity equation is rewritten to

$$m c \frac{dq}{dt} = U_1 A_1 T_1 - U_2 A_2 T_2.$$

Considering adiabatic conditions, our approach is based on the above thermal conductivity equations and can be stated with

$$\frac{dT}{dt} = \frac{U_1 A_1}{m c \Delta S} T_1 - \frac{U_2 A_2}{m c \Delta S} T_2 \Leftrightarrow \frac{dT}{dt} = p_1 \cdot T_1 - p_2 \cdot T_2 \text{ with } T_1 > T > T_2, \quad (3)$$

where  $m$  is the mass in (kg),  $c$  the specific heat capacity in (J/kg K),  $U_i$  the heat transfer coefficient in (W/m<sup>2</sup> K) and  $A_i$  the area in (m<sup>2</sup>).  $\Delta S$  represents the change rate of entropy. In the right part of (3), parameters  $p_1$  and  $p_2$  summarize all unknown material properties and the presumed constant entropy change rate. The temperature  $T$  lies in x-direction between  $T_1$  and  $T_2$ . The exact position is unknown, but stays constant. Thus, the room temperature can be modelled as shown in Fig. 4.

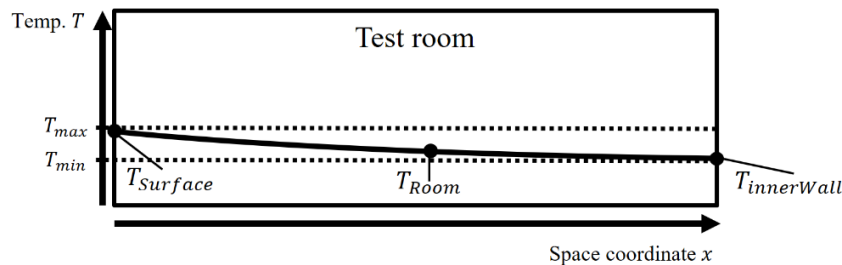


Fig. 4: One-dimensional heat transfer model

Derived from (3), the test room temperatures can be modeled as a linear 8<sup>th</sup> order ordinary different equation (ODE), using the test room structure given in Fig. 2.

$$\begin{aligned}
\frac{dT_{Core}}{dt} &= p_1 \cdot q_{In} - p_2 \cdot \Delta T_A \\
\frac{dT_2}{dt} &= p_3 \cdot \Delta T_A - p_4 \cdot \Delta T_B \\
\frac{dT_{Surface}}{dt} &= p_5 \cdot \Delta T_B - p_6 \cdot \Delta T_C \\
\frac{dT_{Room}}{dt} &= p_7 \cdot \Delta T_C - p_8 \cdot \Delta T_D \\
\frac{dT_5}{dt} &= p_9 \cdot \Delta T_D - p_{10} \cdot \Delta T_E \\
\frac{dT_{innerWall}}{dt} &= p_{11} \cdot \Delta T_E - p_{12} \cdot \Delta T_F \\
\frac{dT_7}{dt} &= p_{13} \cdot \Delta T_F - p_{14} \cdot \Delta T_G \\
\frac{dT_{outerWall}}{dt} &= p_{15} \cdot \Delta T_G - p_{16} \cdot \Delta T_H
\end{aligned} \tag{3}$$

whereby  $\Delta T_A$  to  $\Delta T_H$  represents temperature gradients, which are causative for the energy transfer. This is a simplified model, because expansion of the space and wall due to temperature change and non-isotropic conditions are not taken into account. Moreover, this ODE is a linear model and does not model convective heat transfer nor radiation, which results in ODEs of third respectively fourth order. This model assumes thermal conduction as the predominant heat transfer method. In further research, a nonlinear heat transfer differential equation could be investigated to reduce this modelling error.

In the given ODE system (4) surface and room temperature are coupled directly due to the direct temperature influence of the night storage heater's surface temperature to the average room temperature. All other temperature couplings are done with an additional state variable in between. Thus, this temperature coupling, which is using two differential equations, can be understood as an LTI system of second order, which is able to store thermal energy.

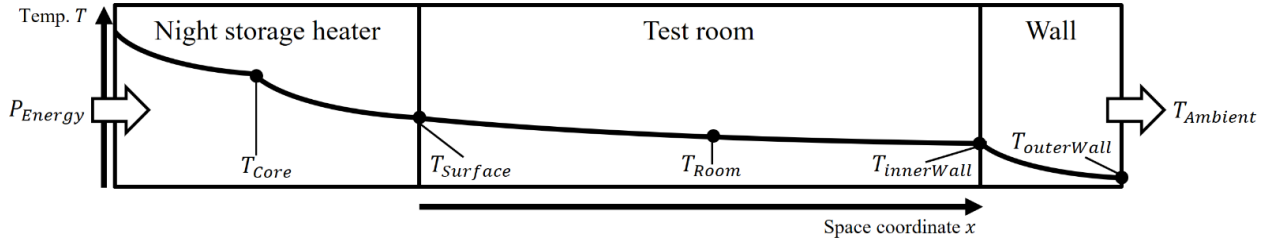


**Fig. 5: Test Room with Placement of Temperature and Heat Transfer Measuring Points**

The reduction of unknown or uncertain parameters can be done by reformulation the ODE system (4) the same way as in the right hand side of (3). With the states  $x_1 = x_{Core}$ ,  $x_3 = x_{Surface}$ ,  $x_4 = x_{Room}$ ,  $x_6 = x_{innerWall}$  and  $x_8 = x_{outerWall}$  and facilitating (4), the heat transfer and its temperature coupling is derived by

$$\begin{aligned}
\dot{x}_{Core} &= \dot{x}_1 = p_1 \cdot P_{Energy}(t) - p_2(x_{Core} - x_2) \\
\dot{x}_2 &= p_3(x_{Core} - x_2) - p_4(x_2 - x_{Surface}) \\
\dot{x}_{Surface} &= \dot{x}_3 = p_5(x_2 - x_{Surface}) - p_6(x_{Surface} - x_{Room}) \\
\dot{x}_{Room} &= \dot{x}_4 = p_7(x_{Surface} - x_{Room}) - p_8(x_{Room} - x_5) \\
\dot{x}_5 &= p_9(x_{Room} - x_5) - p_{10}(x_5 - x_{innerWall}) \\
\dot{x}_{innerWall} &= \dot{x}_6 = p_{11}(x_5 - x_{innerWall}) - p_{12}(x_{innerWall} - x_7) \\
\dot{x}_7 &= p_{13}(x_{innerWall} - x_7) - p_{14}(x_7 - x_{outerWall}) \\
\dot{x}_{outerWall} &= \dot{x}_8 = p_{15}(x_7 - x_{outerWall}) - p_{16}(x_{outerWall} - T_{Ambient}(t))
\end{aligned} \tag{5}$$

This ODE system can be rewritten in state-space representation

$$\dot{\underline{x}}(t) = \underline{A} \underline{x}(t) + \underline{B} \underline{u}(t), \underline{x}(0) = \underline{x}_0, \underline{x} \in \mathbb{R}^8, \underline{A} \in \mathbb{R}^{8 \times 8}, \underline{B} \in \mathbb{R}^{8 \times 2}, \underline{u} \in \mathbb{R}^2. \tag{6}$$

Hereby, system matrix  $\underline{A}$  and input matrix  $\underline{B}$  consists of parameters  $p_1$  to  $p_{16}$ , and input vector  $\underline{u}(t) = (P_{Energy}(t); T_{Ambient}(t))^T$  contains time variant signals of electrical power and ambient temperature. The solution of (5) can be derived from

$$\underline{x}(t) = e^{\underline{A}t} \underline{x}_0 + e^{\underline{A}t} \int_0^t e^{-\underline{A}\tau} \underline{B} \underline{u}(\tau) d\tau \quad (7)$$

but solving the integral on the right hand side is very difficult and cannot be done without further investigation in the wide field of control theory. Thus, this system is solved numerically using ODE45-solver of Matlab [7,8].

The initial temperatures for solving (5) are set to

$$\underline{x}_0 = \underline{x}(0) = \begin{pmatrix} 104.3113403320 \\ 98.1622664268 \\ 29.6006927490 \\ 20.1605898539 \\ 17.6835182491 \\ 14.9594917297 \\ 12.5007693350 \\ 8.2465286255 \end{pmatrix} \text{ } ^\circ\text{C}.$$

Solving ODE (5) leads to numerical solutions  $f_1$  to  $f_5$ , which represent time discrete series of temperatures of

$$\begin{aligned} x_{Core}(t_k; \underline{p}) &= x_1(t_k; \underline{p}) = f_1(t_k; \underline{p}, P_{Energy}, T_{Ambient}) \\ x_{Surface}(t_k; \underline{p}) &= x_2(t_k; \underline{p}) = f_2(t_k; \underline{p}, P_{Energy}, T_{Ambient}) \\ x_{Room}(t_k; \underline{p}) &= x_3(t_k; \underline{p}) = f_3(t_k; \underline{p}, P_{Energy}, T_{Ambient}) \\ x_{innerWall}(t_k; \underline{p}) &= x_4(t_k; \underline{p}) = f_4(t_k; \underline{p}, P_{Energy}, T_{Ambient}) \\ x_{outerWall}(t_k; \underline{p}) &= x_5(t_k; \underline{p}) = f_5(t_k; \underline{p}, P_{Energy}, T_{Ambient}) \end{aligned} \quad (8)$$

depending on the unknown parameters  $p_1$  to  $p_{16}$  and the known time variant input data  $P_{Energy}(t)$  and  $T_{Ambient}(t)$ .

A least squares method [1] is applied for estimating the sixteen parameters by fitting ODE solutions to the experimental data measured during the nine-day test run. In general, the parameter estimation is gathered by applying an unconstrained optimization problem [7] as

$$\underline{p}^* = \underset{\underline{p}}{\operatorname{argmin}} \sum_{k=1}^{k_{max}} \left( x_{Measure}(k) - x_{Model}(k; \underline{p}) \right)^2, \quad (9)$$

whereby  $k_{max}$  represents the count of all measurements and  $k$  itself the  $k$ th measurement. Empirical data is stored in  $x_{Measure}(k)$  and the model output  $x_{Model}(k; \underline{p})$  depends on the unknown parameters  $\underline{p}$ . The given problem of modeling the temperatures an energy flow on a night storage heaters provides five temperature time series and an unknown parameter set with  $\underline{p} \in \mathbb{R}^{16}$ . Thus, parameter estimation is noted with

$$\underline{p}^* = \underset{\underline{p}}{\operatorname{argmin}} \sum_{k=1}^{k_{max}} \left( x_{Measure,Core}(t_k) - x_{Core}(t_k; \underline{p}, P_{Energy}, T_{Ambient}) \right)^2 \quad (10a)$$

$$+ \sum_{k=1}^{k_{max}} \left( x_{Measure,Surface}(t_k) - x_{Surface}(t_k; \underline{p}, P_{Energy}, T_{Ambient}) \right)^2 \quad (10b)$$

$$+ 2 \cdot \sum_{k=1}^{k_{max}} \left( x_{Measure,Room}(t_k) - x_{Room}(t_k; \underline{p}, P_{Energy}, T_{Ambient}) \right)^2 \quad (10c)$$

$$+ \sum_{k=1}^{k_{max}} \left( x_{Measure,innerWall}(t_k) - x_{innerWall}(t_k; \underline{p}, P_{Energy}, T_{Ambient}) \right)^2 \quad (10d)$$

$$+ \sum_{k=1}^{k_{max}} \left( x_{Measure,outerWall}(t_k) - x_{outerWall}(t_k; \underline{p}, P_{Energy}, T_{Ambient}) \right)^2 \quad (10e)$$

which represents the computation of the Gaussian  $L_2$  norm summed up over all five measurement time series and over all temperature measuring points of time  $k_{max}$ . The room temperature is weighted with a double rate, because this is the target model output for latter computations.

The target function (right hand side of (10)) is neither a linear nor a convex function, thus, identifying the optimal parameter set providing the guaranteed lowest target function output of the least squares computation was not achieved in this contribution. Identifying a parameter set providing a sufficient low target function output was reached by computing stepwise a smaller ODE system, which also reduce the parameter set to the size of four parameters. Thus, the first parameter estimation for  $p_1$  to  $p_4$  is computed by applying the ODE system

$$\begin{aligned}\dot{x}_{Core}(t) = \dot{x}_1(t) &= p_1 \cdot P_{Energy}(t) - p_2(x_{Core}(t) - x_2(t)) \\ \dot{x}_2(t) &= p_3(x_{Core}(t) - x_2(t)) - p_4(x_2(t) - T_{Surface}(t))\end{aligned}$$

to (10a). Hereby the given measurements of the surface temperature  $T_{Surface}(t)$  are used as one of the time variant parameters. The same approach is applied for identifying  $p_5$  and  $p_6$  using ODEs

$$\dot{x}_{Surface}(t) = \dot{x}_3(t) = p_5(x_2(t) - x_{Surface}(t)) - p_6(x_{Surface}(t) - T_{Room}(t))$$

and computing the optimal parameters with (10b). This method is repeated for  $p_7$  to  $p_9$  using the ODE system

$$\begin{aligned}\dot{x}_{Room}(t) = \dot{x}_4(t) &= p_7(T_{Surface}(t) - x_{Room}(t)) - p_8(x_{Room}(t) - x_5(t)) \\ \dot{x}_5(t) &= p_9(x_{Room}(t) - x_5(t)) - p_{10}(x_5(t) - T_{InnerWall}(t))\end{aligned}$$

with (10c). Moreover, the parameters  $p_{11}$  to  $p_{14}$  are identified with

$$\begin{aligned}\dot{x}_{InnerWall}(t) = \dot{x}_6(t) &= p_{11}(x_5(t) - x_{InnerWall}(t)) - p_{12}(x_{InnerWall}(t) - x_7(t)) \\ \dot{x}_7(t) &= p_{13}(x_{InnerWall}(t) - x_7(t)) - p_{14}(x_7(t) - T_{OuterWall}(t))\end{aligned}$$

together with (10d). And, finally, the last two parameters  $p_{15}$  and  $p_{16}$  are computed with

$$\dot{x}_{OuterWall}(t) = \dot{x}_8(t) = p_{15}(x_7(t) - x_{OuterWall}(t)) - p_{16}(x_{OuterWall}(t) - T_{Ambient}(t))$$

and a parameter estimation using (10e). With this, the best computed parameter set  $p^*$  is derived from the above described stepwise local optimization algorithm provided by Matlab's Optimization Toolbox [3] with

$$\underline{p}^* = \begin{pmatrix} 7.711390906572707 \cdot 10^{-6} \\ 5.070895673299722 \cdot 10^{-4} \\ 1.279915574253624 \cdot 10^{-2} \\ 3.179727995259820 \cdot 10^{-4} \\ 1.024185195967078 \cdot 10^{-4} \\ 7.886733957407758 \cdot 10^{-4} \\ 2.610319575218490 \cdot 10^{-5} \\ 3.151320103865306 \cdot 10^{-4} \\ 1.273220737747616 \cdot 10^{-4} \\ 3.988458075696419 \cdot 10^{-5} \\ 6.254330656917015 \cdot 10^{-4} \\ 7.956221589171986 \cdot 10^{-4} \\ 1.011355181029409 \cdot 10^{-4} \\ 7.867464077439637 \cdot 10^{-5} \\ 1.273220737747612 \cdot 10^{-3} \\ 2.017918879756508 \cdot 10^{-3} \end{pmatrix}.$$

The time series of core, surface, room, inner and outer wall temperature is now computed with the above identified parameter set. Simulations of these temperatures over nine days are plotted in Fig. 6.

We have to express, that this result is not the global minimum for the nonlinear optimization problem in (10). The here given parameter set could be a local minimum. There are some methods to solve this problem globally. An interval arithmetic approach [6] could be applied to compute the global optimum and its optimal parameter set.

A direct comparison of the measured room temperature and the modeled room temperature is shown in Fig. 6. At the beginning the modeled temperature drops due to the predetermined initial conditions. The aberration of the modeled temperature from the measured could be caused by the above mentioned modelling errors. Even it looks flawed in the first hours of the nine-day simulation period, this temperature model results from best found parameter set.

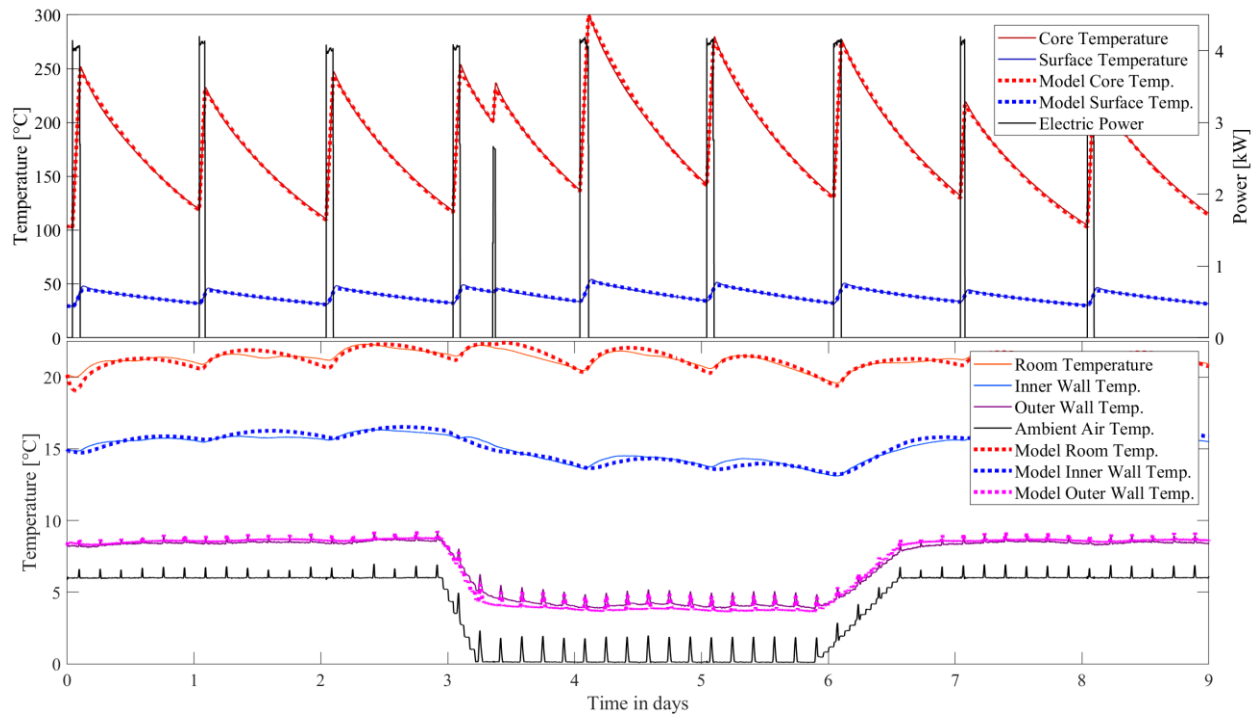


**Fig. 6: Modeling Results versus Temperature Measurement**

The repeated increase in the course of measured room temperature at noon results from additional heat input from the sun, which heats up the technical center in which the test room is located. Here, if the temperature in the technical center deviates by more than three Kelvin from the test room's temperature, an effect on the temperature in test room is visible. This second order measurement error has meanwhile remedied by an additional air conditioning unit in the technical center and the previous investigation will be repeated in further test runs.

## Results

The computed results of a nine-day simulation period are shown in Fig. 6 and Fig. 7, whereas the room temperature maximum deviation is 0.96 Kelvin and the average deviation is 0.21 Kelvin (see Fig. 7). This represents an excellent result, considering the length of its underlying nine-day simulation period, disturbances, the relaxed modelling approach and its modelling errors.

Furthermore, the room temperature is simulated for two months with the specification of ambient air temperature for January of 2017 as a winter month and July of 2017 as a summer month. A permissible lower limit of the room temperature of 20 degrees Celsius was defined as a constraint for a 15-minute look-ahead algorithm, which sets a charging signal, if the room temperature could drop below the given lower limit starting from the actual temperature. The computed results are shown in Fig. 8 and Fig. 9. In both cases the night storage heater is charged at regular intervals, whereby the lower limit room temperature of 20 degrees Celsius is never violated. Charging the night storage heater often occurs, although it would not be necessary with the given limit. Thus, the room temperature often rises unnecessarily and results in a wide fluctuation range. The definition of a second upper limit for the room temperature could avoid this charging events.

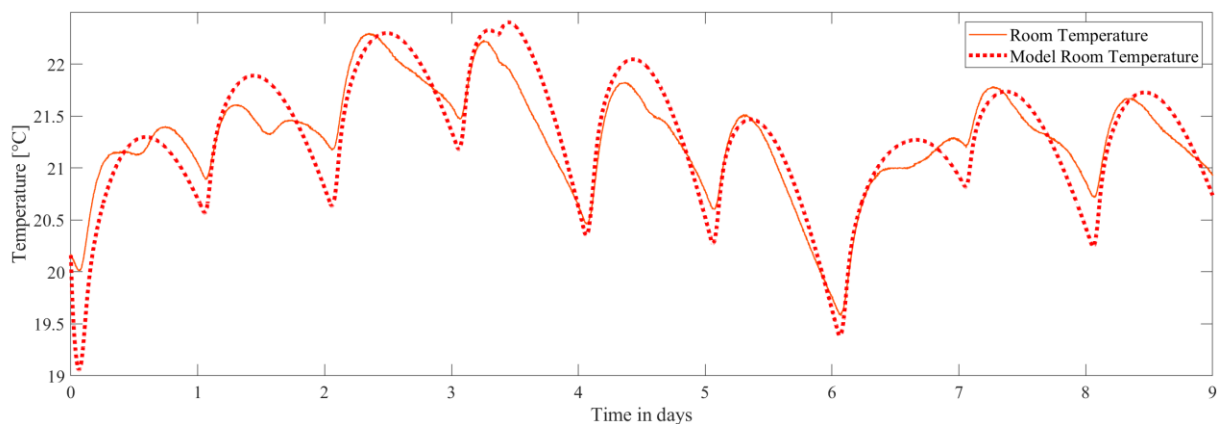


**Fig. 7: Detailed Room Temperature Measurement and Modeling Results**

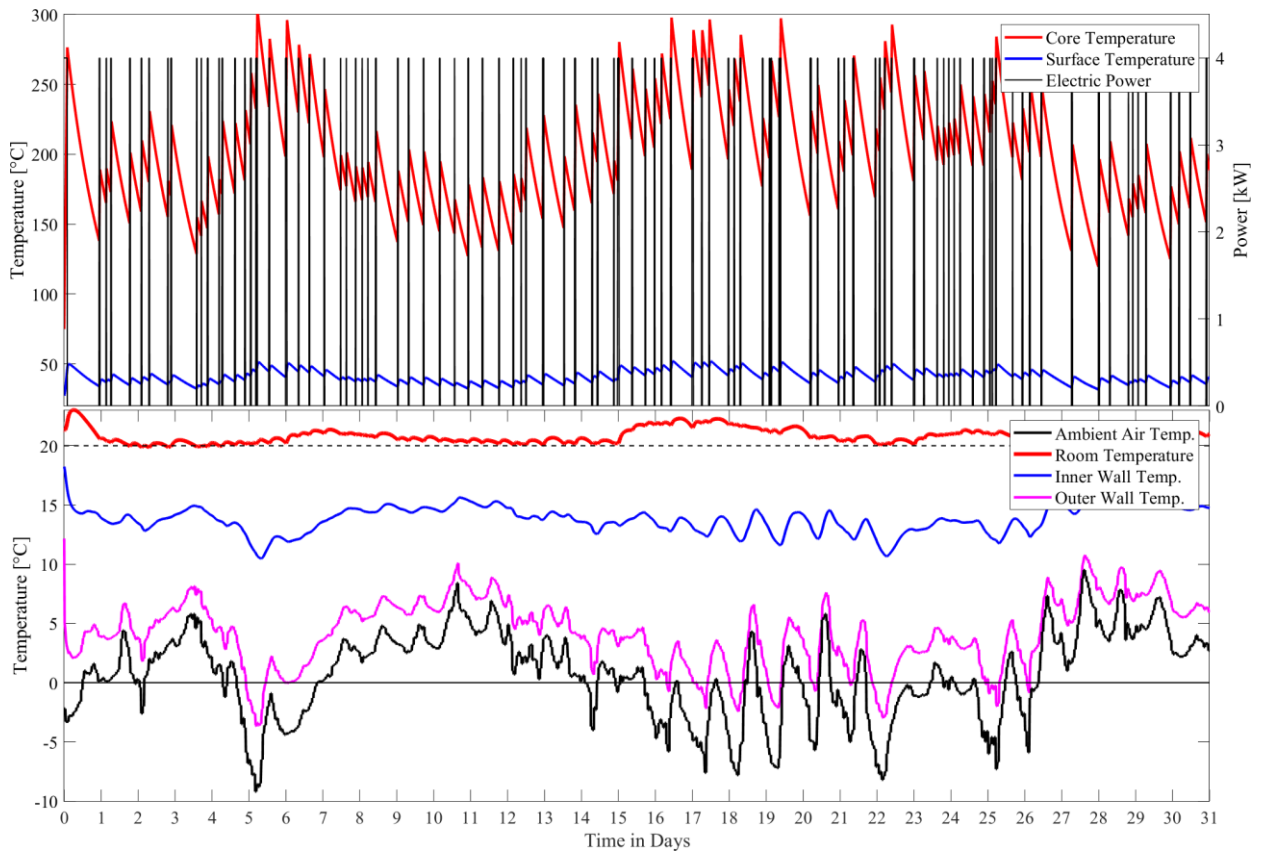


**Fig. 8: Simulation over 31 Days in January with Ambient Temperatures of 2017**

With the two limits, an upper and a lower bound for room temperature, it would be possible to keep the temperature within a small temperature range. In this way, additional heat input can be prevented and in order to that maybe energy saved.

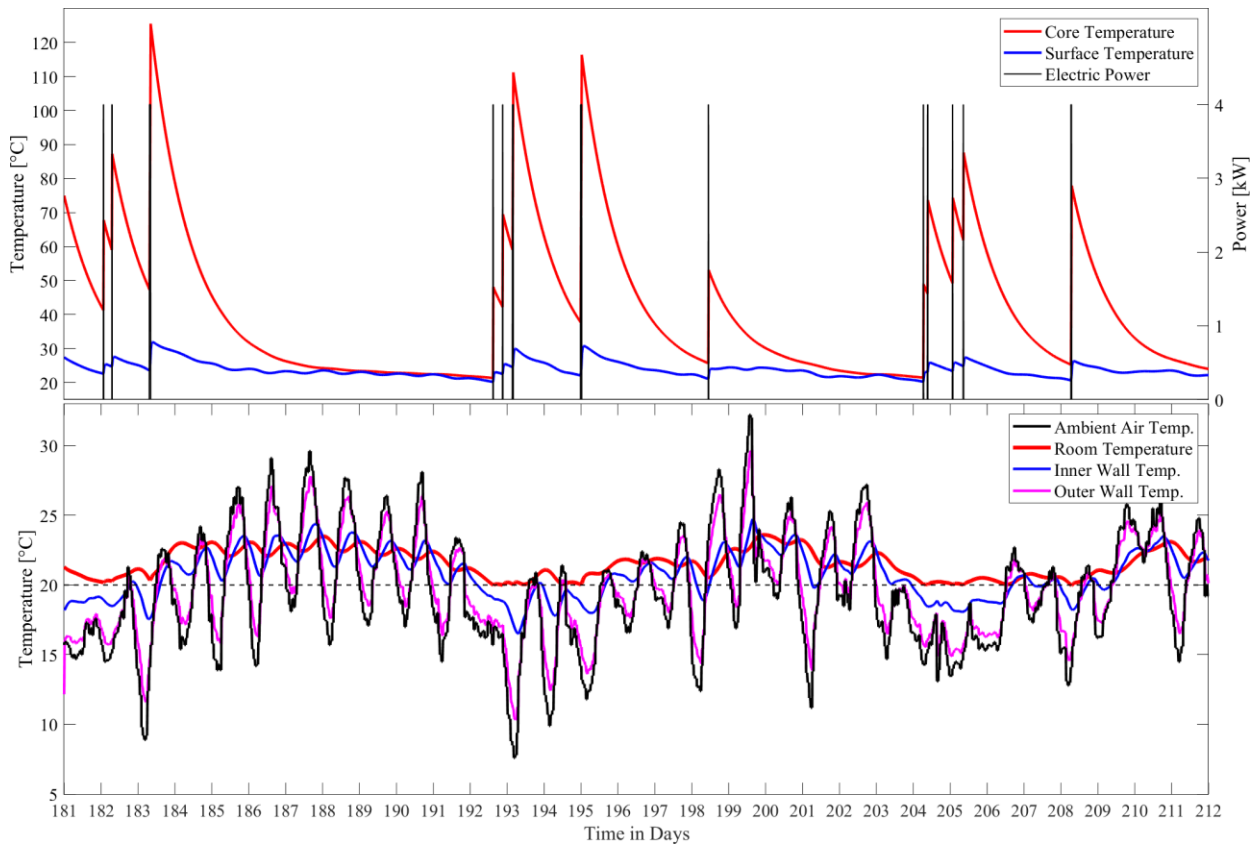


**Fig. 9: Simulation over 31 Days in July with Ambient Temperatures of 2017**

During the summer months, in general it is not necessary to operate night storage heaters, because the 24h-hour-average ambient air temperature is located above a recommended limit for heating, which is usually set to 18 degrees Celsius. In this summer month simulation, there are some days in which the room temperature could drop below the lower bound, which can be seen in Fig. 8. For this reason, the night storage heater charged a few times in the summer month. In July the problem with the rising room temperature above the defined limit due to charging is less pronounced than in winter month and occurs only by the additional heat input from rising ambient air temperature.

## Conclusions

In this contribution a method is presented to simulate the temporal room temperature solving ODEs. Parameter estimation provides unknown parameters of the ODE-model by fitting the model output to real measurement data, whereby the given electric power consumption and outside ambient temperature are time variant data series.

With the presented method the room temperature for a given test room is computed depending on night storage heater's energy supply and predetermined outside ambient temperature, which can be provided by meteorological service providers. This facilitate the computation of controlled energy supply periods to comply with the temperature requirements in the test room.

In a second step this method enables the possibility to detect and define optimal charging times. It allows to operate night storage heaters more flexible and even offers the opportunity to integrate them into the energy market. Following this, it is possible e. g. to charge the night storage heaters, if a surplus of renewable energy is available, or not to charge them if an overload in the power grid threatens. Finally, this method of temperature modelling could also be applied to other scheduled loading and unloading problems or energy storage challenges.

In further research room temperature will be restricted to lower an upper bounds by controlling the electrical power input. Thereby the charging releases will be extended to the entire day instead of the conventional charging releases for electric night storage heaters at night like shown in the first simulation for one winter and one summer month with set lower limit. A further step will be the additional integration of electricity prices to determine optimal charging times taking into account to the electricity procurement costs.

## References

- [1] Åström, K. J., & Eykhoff, P. (1971). System identification—a survey. *Automatica*, 7(2), 123-162.
- [2] German Meteorological Service (2017). Historic Climate Data Station No. 10400 Düsseldorf, Deutscher Wetterdienst (DWD), Offenbach. URL <https://www.dwd.de/DE/leistungen/klimadatendeutschland/klarchivstunden.html?nn=16102>, visited on 21<sup>st</sup> May 2021.
- [3] Embaye, M., Al-Dadah, R. K., & Mahmoud, S. (2016). Effect of flow pulsation on energy consumption of a radiator in a centrally heated building. *International Journal of Low-Carbon Technologies*, 11(1), 119-129.
- [4] Farid, M. M., Khudhair, A. M., Razack, S. A. K., & Al-Hallaj, S. (2004). A review on phase change energy storage: materials and applications. *Energy conversion and management*, 45(9-10), 1597-1615.
- [5] Graßmann, A., Peters, F. (1999). Experimental investigation of heat conduction in wet sand, *Heat and Mass Transfer* 35, 289-294, Springer.
- [6] Gennat, M. and Tibken, B. (2008). Computing guaranteed bounds for uncertain cooperative and monotone nonlinear systems. IFAC World Congress 2008, Seoul, Korea. IFAC Proceedings Volumes, 41(2), 4846-4851.
- [7] Shampine, L. F., & Reichelt, M. W. (1997). The matlab ode suite. *SIAM journal on scientific computing*, 18(1), 1-22.
- [8] The MathWorks (2018). Matlab and optimization toolbox release 2018a. URL <https://www.mathworks.com/products/matlab.html>, visited on 21<sup>st</sup> May 2021.